JOURNAL OF AGRICULTURAL AND FOOD CHEMISTRY

Article

pubs.acs.org/JAFC

Spectroscopic Studies of DNA Interactions with Food Colorant Indigo Carmine with the Use of Ethidium Bromide as a Fluorescence Probe

Yadi Ma, Guowen Zhang,* and Junhui Pan

State Key Laboratory of Food Science and Technology, Nanchang University, Number 235, Nanjing East Road, Nanchang 330047, Jiangxi, People's Republic of China

ABSTRACT: The interaction of indigo carmine (IC) with calf thymus DNA in physiological buffer (pH 7.4), using ethidium bromide (EB) dye as a fluorescence probe, was investigated by ultraviolet−visible absorption, fluorescence, and circular dichroism (CD) spectroscopy, coupled with viscosity measurements and DNA-melting studies. Hypochromicity of the absorption spectra of IC and enhancement in fluorescence polarization of IC were observed with the addition of DNA. Moreover, the binding of IC to DNA was able to decrease iodide and single-stranded DNA (ssDNA) quenching effects, increase the melting temperature and relative viscosity of DNA, and induce the changes in CD spectra of DNA. All of the evidence indicated that IC interacted with DNA in the mode of intercalative binding. Furthermore, the three-way synchronous fluorescence spectra data obtained from the interaction between IC and DNA−EB were resolved by parallel factor analysis (PARAFAC), and the results provided simultaneously the concentration information and the pure spectra for the three reaction components (IC, EB, and DNA−EB) of the system at equilibrium. This PARAFAC demonstrated that the intercalation of IC molecules into DNA proceeded by substituting for EB in the DNA−EB complex. The calculated thermodynamic parameters, ΔH° and ΔS°, suggested that both hydrophobic interactions and hydrogen bonds played a predominant role in the binding of IC to DNA.

KEYWORDS: *Indigo carmine, calf thymus DNA, spectroscopy, parallel factor analysis, ethidium bromide*

INTRODUCTION

Indigo carmine (IC, structure shown in Figure 1), a synthetic indigoid dye, has been widely used as a coloring agent in food,

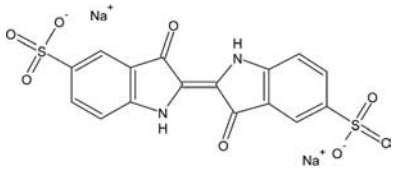

Figure 1. Molecular structure of IC.

such as bread, fruit juices, dairy and skim milk products, tomato catsup, smoked fish, and sweets.[1] This colorant can improve appearance, color, and texture of food products and maintain the natural color during process or storage. Nevertheless, IC is considered as a highly toxic indigoid dye, which can inflict permanent injury to cornea and conjunctiva and generate irritation to the respiratory tract with coughing and shortness of breath.[2] When administered intravenously to determine the potency of the urinary collecting system, it is also known to arouse mild to severe hypertension and cardiovascular and respiratory effects in patients.[3] In addition, excess intake of the colorant has been proven to be mutagenic and can cause tumors;[4,5] thus, IC may have the potential to increase genetic damage in future human populations. In view of the above safety threats, much more safety assessment of IC should be confirmed and the use of this colorant should be thoroughly controlled by laws, regulations, and acceptable daily intake (ADI) values.

Deoxyribonucleic acid (DNA) is an important genetic substance in the organism, which plays an extremely significant role in the process of human life. It carries most of the hereditary information and facilitates the biological synthesis of proteins and enzymes through replication and transcription of this information.[6] DNA is frequently the main molecular target for natural and synthetic organics. Amounts of poisonous chemicals, such as organic dyes, heavy metals, pesticides, etc., enter into the body by inhalation, ingestion, or absorption through the skin. They can interact with DNA directly or indirectly *in vivo*, which may change the DNA structure and induce DNA damage, eventually affecting its function or genetic expression.[7] Kashanian et al. have investigated the interaction between tartrazine and calf thymus DNA (ctDNA) using Hoechst 33258 as a fluorescence probe. Their results indicated that tartrazine bound to ctDNA via a groove binding mode and the colorant had a toxic potential to ctDNA *in vitro*.[8] Therefore, the studies on the interaction of food colorant IC with DNA are of great significance, which could provide useful information for further discussion of the toxicology of the dye.

A number of techniques have been used to study the binding properties between small molecules and DNA, including electrochemistry,[9] fluorescence spectroscopy,[10] ultraviolet−visible (UV−vis) spectrophotometry,[11] circular dichroism (CD),[12] nuclear magnetic resonance,[13] and mass spectrometry.[14] Among these, spectroscopic techniques offer the

Received: August 27, 2012
Revised: October 11, 2012
Accepted: October 12, 2012
Published: October 12, 2012

dx.doi.org/10.1021/jf303698k | J. Agric. Food Chem. 2012, 60, 10867−10875

advantages of high sensitivity, reproducibility, selectivity, and convenience. However, for complex systems of more than two components, it is difficult to distinguish these existing species because their response signals often overlap. A well-known soft modeling algorithm, parallel factor analysis (PARAFAC),[15] has been introduced to overcome this restriction. The PARAFAC method can provide the concentration profiles and pure spectra of all of the chemically analyzed components. The concentration profiles afford the information on the mechanism of the reaction process, while the features of the recovered pure spectra help to identify the species involved.

In the present work, the binding mode and thermodynamic characteristics between the food colorant IC and ctDNA were investigated with the aid of ethidium bromide (EB) as a molecular probe, using fluorescence, UV−vis absorption, and CD spectroscopy, as well as DNA-melting temperature and viscosity measurements. Furthermore, PARAFAC modeling, a chemometrics approach, was applied to decompose the three-way synchronous fluorescence data array of the competitive interaction between IC and the EB probe with DNA to explore the changes and progress of the complicated reaction system.

MATERIALS AND METHODS

Materials. ctDNA was purchased from Sigma-Aldrich Co. (St. Louis, MO) and dissolved in ultrapure water containing 0.1 mol L^{-1} NaCl. The purity of DNA was checked by monitoring the ratio of the absorbance at 260/280 nm, and the solution gave the ratio of A_{260}/A_{280} = 1.86, indicating that DNA was sufficiently free from protein.[16] The concentration of DNA in stock solution was determined to be 1.92×10^{-3} mol L^{-1} by UV absorption at 260 nm using a molar absorption coefficient ε_{260} = 6600 L mol^{-1} cm^{-1}.[17] IC (purity > 96.0%) was obtained from Sinopharm Chemical Reagent Co., Ltd. (Shanghai, China), and the stock solution (1.50×10^{-3} mol L^{-1}) of IC was prepared in ultrapure water. The stock solution (1.00×10^{-3} mol L^{-1}) of EB (Sigma-Aldrich Co., St. Louis, MO) was made up by dissolving its crystals in ultrapure water. All solutions were adjusted with 0.05 mol L^{-1} Tris-HCl buffer of pH 7.4. All chemicals were of analytical reagent grade, and ultrapure water was used throughout the experiment.

Instrumentations. The fluorescence and synchronous fluorescence spectra were performed with the use of a 1.0 cm quartz cell on a Hitachi spectrofluorimeter model F-4500 (Hitachi, Japan) equipped with a 150 W xenon lamp and a thermostat bath. UV−vis absorption spectra were measured on a Shimadzu UV-2450 spectrophotometer (Shimadzu, Japan) using a 1.0 cm cell. CD spectra were recorded on a Bio-Logic MOS 450 CD spectrometer (Bio-Logic, France) using a 1.0 mm path length quartz cuvette. The viscosity measurements were carried out using a NDJ-79 viscometer (Yinhua Flowmeter Co., Ltd., Hangzhou, China). An electronic thermostat water bath (Shanghai Yuejin Medical Instrument Company, Shanghai, China) was used for controlling the temperature. A pHS-3C digital pH meter (Shanghai Exact Sciences Instrument Co. Ltd., Shanghai, China) was used to detect the pH values of the aqueous solutions. A Millipore Simplicity water purification system (Millipore, Molsheim, France) was applied to produce fresh ultrapure water. All experiments, unless specified otherwise, were carried out at room temperature.

Fluorescence Measurements. A 3.0 mL solution containing 6.0×10^{-5} mol L^{-1} IC was added to a 1.0 cm quartz cuvette and then titrated by successive addition of the 9.60×10^{-4} mol L^{-1} DNA solution with a trace syringe (to give a final concentration of 3.097×10^{-5} mol L^{-1}). These solutions were allowed to stand for 6 min to equilibrate, and the fluorescence spectra were then recorded at four temperatures (293, 298, 303, and 310 K) in the wavelength range of 290−490 nm, with exciting wavelength at 280 nm. The widths of both the excitation and emission slits were set at 5.0 nm. The appropriate blanks corresponding to the Tris-HCl buffer solution were subtracted to correct the background of the fluorescence.

To eliminate the possibility of re-absorption and inner filter effect arising from UV absorption, the fluorescence data were corrected for absorption of excitation light and emitted light according to following relationship:[18]

$$F_c = F_m \, e^{(A_1 + A_2)/2} \quad (1)$$

where F_c and F_m are the corrected and measured fluorescence, respectively. A_1 and A_2 are the absorbance of DNA at excitation and emission wavelengths, respectively. The intensity of fluorescence used in this paper was the corrected fluorescence intensity.

The competitive interaction between IC and EB dye with DNA was implemented as follows: fix the concentrations of EB at 5.0×10^{-6} mol L^{-1} and DNA at 5.5×10^{-5} mol L^{-1}, respectively, and then titrate with increasing amounts of IC solution (the number for adding the colorant was 14). After these solutions had been allowed to stand for 6 min to equilibrate, the three-way synchronous fluorescence measurements were carried out over a excitation wavelength range of 200−700 at 1 nm intervals (total 501 wavelengths) and $\Delta\lambda$ (a constant wavelength distance between emission and excitation wavelengths) was changed in the range of 10−200 at 10 nm intervals (total number of $\Delta\lambda$ increments was 20). The data were arranged in an $I \times J \times K$ three-way array, where the first index (I) referred to the $\Delta\lambda$ wavelengths, the second index (J) referred to the excitation wavelengths, and the third index (K) referred to the samples. Thus, the dimension of the experimental three-way array was $20 \times 501 \times 14$.

Fluorescence Polarization Experiments. Fluorescence polarization experiments were measured by keeping the concentration of IC at 6.0×10^{-5} mol L^{-1} while varying DNA concentrations from 0 to 3.097×10^{-5} mol L^{-1}. The samples were performed on a Hitachi spectrofluorimeter model F-4500 at the corresponding excitation and emission wavelengths: 280 and 322 nm, respectively. Both the excitation and emission bandwidths were set at 5.0 nm after setting a pair of polarizers.

UV−Vis Absorption Spectroscopy. The UV−vis absorption spectra of a fixed concentration of IC without and with various concentrations of DNA were measured over a wavelength range of 230−450 nm in pH 7.4 Tris-HCl buffer solution at room temperature. All observed absorption spectra were corrected for the buffer absorbance.

Effects of Single-Stranded DNA (ssDNA) and Double-Stranded DNA (dsDNA). The ssDNA solution was prepared by heating native dsDNA solution in a boiling water bath for 15 min, followed by rapidly cooling in an ice−water bath. When heating gradually up to 298 K, dsDNA becomes ssDNA.[10] A comparison of the quenching effects of ssDNA and dsDNA was performed by successively adding ssDNA or dsDNA solution, respectively, to IC solution at a constant concentration. The fluorescence intensities were measured at an emission wavelength of 322 nm, with an excitation wavelength at 280 nm.

Iodide Quenching Experiments. Fluorescence quenching studies were performed by gradually adding the anionic quencher solution (KI) to IC and DNA−IC complex solutions. The fluorescence spectra of the solutions were recorded, and the quenching constants were then calculated.

Viscosity Measurements. Viscometric titrations were conducted using a viscometer, which was thermostatted at 25 ± 0.1 °C in a thermostatic water bath. The flow time of the solution through the capillary was measured with an accuracy of ±0.20 s using a digital stopwatch. The mean values of five replicated measurements were used to evaluate the average relative viscosity of the samples. The experiments were performed by adding appropriate amounts of IC into the viscometer to give a certain r (r = [IC]/[DNA]) value while fixing the DNA concentration at 3.6×10^{-5} mol L^{-1}. The relative viscosity values of DNA in the presence and absence of IC were calculated from the following equation:[19]

$$\eta/\eta_0 = (t - t_0)/(t_{DNA} - t_0) \quad (2)$$

where t_0 and t_{DNA} are the observed flow time of the buffer and DNA, respectively, while t is the flow time of the DNA−IC complex. The

data have been presented as $(\eta/\eta_0)^{1/3}$ versus the [IC]/[DNA] ratio, where η and η_0 represent the viscosity of DNA in the presence and absence of IC, respectively.

DNA-Melting Studies. The melting temperatures of DNA and the DNA−IC complex were determined by monitoring the absorbance at 258 nm of the samples at different temperatures. The absorbance intensities were then plotted as a function of the temperature ranging from 20 to 100 °C. The values of melting temperatures of DNA and the DNA−IC complex were obtained from the transition midpoint of the melting curves based on f_{ss} versus temperature (T), where $f_{ss} = (A - A_0)/(A_f - A_0)$, where A_0 is the initial absorbance intensity, A is the absorbance intensity corresponding to its temperature, and A_f is the final absorbance intensity.[20]

CD Spectroscopy. CD measurements of DNA and the DNA−IC complex were made at wavelengths between 220 and 320 nm under constant nitrogen flush. The CD spectra of DNA incubated with IC at molar ratios ([IC]/[DNA]) of 0:1, 1:1, and 2:1 were measured in pH 7.4 Tris-HCl buffer solution at room temperature, and the concentration of DNA was kept at 6.0×10^{-4} mol L^{-1}. All observed CD spectra were corrected for the buffer signal, and results were expressed as ellipticity in millidegrees.

Chemometrics: PARAFAC Model. PARAFAC is a chemometrics method for multiway data decomposition based on the so-called trilinear tensor theory,[21] which was used to resolve the three-way array of synchronous fluorescence spectra data obtained from the interaction between IC and the DNA−EB complex. For a trilinear spectral data array with an appropriate number of chosen model factors, PARAFAC will produce unique solutions, corresponding to the true underlying spectra. Additionally, the concentrations of analytes can also be extracted.

The decomposition of a three-way array of synchronous fluorescence data, $\boldsymbol{X}$, with dimensions $I \times J \times K$ is performed. Each PARAFAC component gives three types of loading values: one related to the excitation data (a_h), one related to $\Delta\lambda$ (b_h), and one related to the content of the samples (c_h). Thus, three loadings matrices, $\boldsymbol{A}$, $\boldsymbol{B}$, and $\boldsymbol{C}$ with elements, a_{ih}, b_{jh}, and c_{kh}, can be given for the three dimensions in the data.

The aim is to resolve the three-way array to obtain the three loading matrices. The matrix form of the trilinear model can be expressed by the following equation:

$$x_{ijk} = \sum_{h=1}^{H} a_{ih} b_{jh} c_{kh} + e_{ijk} \tag{3}$$

where x_{ijk} is the original element ($i \rightarrow I$, $j \rightarrow J$, and $k \rightarrow K$) of the trilinear data set $\boldsymbol{X}$, H is the number of fluorescing species, I indicates the number of $\Delta\lambda$, J is the number of excitation wavelength points, K is the number of samples, and e_{ijk} represents a residual error term of the three-way array; $\boldsymbol{E}$ and its sum of squares is minimized.

Alternating least squares (ALS) can be used to find the solution to the PARAFAC model.[22] The method assumes the loadings in two modes and then estimates the unknown set of parameters of the third mode until the residuals of the model are optimized. Hence, if estimates of $\boldsymbol{b}$ and $\boldsymbol{c}$ are given, it is possible to determine $\boldsymbol{a}$ by the least-squares solution to the model, $\boldsymbol{X} = \boldsymbol{a}(\boldsymbol{b} \otimes \boldsymbol{c})$. If the vector $(\boldsymbol{b} \otimes \boldsymbol{c})$ is defined as $\boldsymbol{Z}$ in the case of more than one component, then the model defining $\boldsymbol{A}$ is

$$\boldsymbol{X} = \boldsymbol{A}\boldsymbol{Z} \tag{4}$$

The least-squares estimate of $\boldsymbol{A}$ is

$$\boldsymbol{A} = \boldsymbol{X}\boldsymbol{Z}^T(\boldsymbol{Z}\boldsymbol{Z}^T)^{-1} \tag{5}$$

When the model converges, the results have the same number of triads as the number of factors assumed. Each triad is composed of three orthogonal vectors (column loading vectors $\boldsymbol{a}$, $\boldsymbol{b}$, and $\boldsymbol{c}$) that have the profile of the pure species present in the system. A typical iterative procedure follows the following scheme: (i) estimate the number of chemical components, H, (ii) initialize matrices $\boldsymbol{B}$ and $\boldsymbol{C}$ and estimate $\boldsymbol{A}$ from $\boldsymbol{X}$, $\boldsymbol{B}$, and $\boldsymbol{C}$ by least-squares regression, (iii) estimate matrices $\boldsymbol{B}$ and $\boldsymbol{C}$ in the same way as matrix $\boldsymbol{A}$ in step ii, and (iv) return to step ii until convergence.

RESULTS AND DISCUSSION

Fluorescence Quenching Studies of IC by DNA. Figure 2A illustrates the fluorescence emission spectra of IC with increasing concentrations of DNA. It can be seen from Figure 2A that IC had a strong fluorescence emission peak at 322 nm after being excited at a wavelength of 280 nm and the addition of DNA to IC resulted in a significant reduction in the fluorescence intensity. The results indicated that DNA could interact with IC and quench the intrinsic fluorescence of IC.

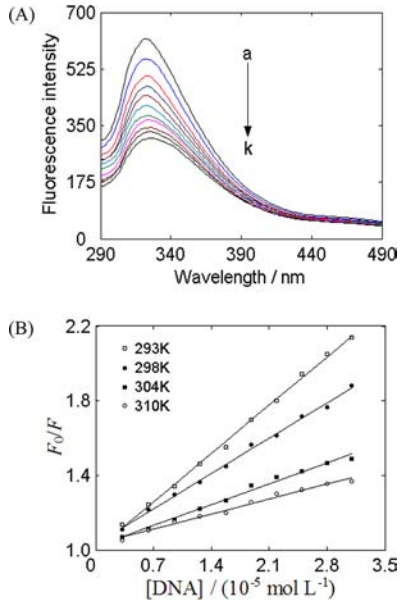

Figure 2. (A) Fluorescence spectra of IC in the absence and presence of DNA (pH 7.4, T = 298 K, λ_{ex} = 280 nm, and λ_{em} = 322 nm). c(IC) = 6.0×10^{-5} mol L^{-1}, and c(DNA) = 0, 0.319, 0.636, 0.950, 1.263, 1.574, 1.882, 2.189, 2.494, 2.796, and 3.097×10^{-5} mol L^{-1}, corresponding to the curves from a to k, respectively. (B) Stern−Volmer plots for the fluorescence quenching of IC by DNA at different temperatures.

Fluorescence quenching is a very common phenomenon, which refers to a decrease of the quantum yield of fluorescence from a fluorophore because of a variety of molecular interactions, including excited-state reactions, molecular rearrangements, energy transfer, ground-state complex formation, and collisional quenching. The different mechanisms of quenching are usually classified as either dynamic or static quenching. One current method to distinguish dynamic and static is by their different dependence upon the temperature. For static quenching, the quenching constant decreases with an increasing temperature, but the reverse effect would be observed for dynamic quenching.[23]

To study the quenching mechanism between DNA and IC, the fluorescence quenching data were analyzed by the Stern−Volmer equation:[23]

$$\frac{F_0}{F} = 1 + K_{SV}[Q] = 1 + K_q\tau_0[Q] \tag{6}$$

where F_0 and F are the fluorescence intensities in the absence and presence of DNA, respectively. K_{SV} is the Stern−Volmer quenching constant, which was determined by linear regression

Table 1. Quenching Constants (K_{SV}), Binding Constants (K_a), and Relative Thermodynamic Parameters for the Interaction of IC with DNA at Different Temperatures

T (K)	K_{SV} ($\times 10^4$, L mol^{-1})	R^a	K_a ($\times 10^4$, L mol^{-1})	R^b	$\Delta H°$ (kJ mol^{-1})	$\Delta G°$ (kJ mol^{-1})	$\Delta S°$ (J mol^{-1} K^{-1})
293	3.70 ± 0.01	0.9989	5.35 ± 0.06	0.9973	−23.36 ± 0.02	−26.53 ± 0.40	10.81 ± 0.06
298	2.70 ± 0.01	0.9984	4.58 ± 0.04	0.9992		−26.58 ± 0.12	
304	1.60 ± 0.01	0.9957	3.77 ± 0.17	0.9947		−26.65 ± 0.21	
310	1.15 ± 0.01	0.9933	3.17 ± 0.11	0.9985		−26.71 ± 0.54	

$^a R$ is the correlation coefficient for the K_{SV} values. $^b R$ is the correlation coefficient for the K_a values.

of a plot of F_0/F against $[Q]$. K_q is the quenching rate constant of the biomolecule. τ_0 is the average lifetime of the fluorophore without a quencher; the value of τ_0 of the biopolymer is 10^{-8} s.[24] $[Q]$ is the concentration of DNA.

The curves of F_0/F versus $[Q]$ at four different temperatures (293, 298, 304, and 310 K) are displayed in Figure 2B. The linear plots suggested that only one type of quenching process occurred, in either static or dynamic quenching. The corresponding K_{SV} values for the interaction between IC and DNA are presented in Table 1. The results showed that the values of K_{SV} decreased with the increase in the temperature, and the values of K_q were obtained to be $3.70 \pm 0.01 \times 10^{12}$, $2.70 \pm 0.01 \times 10^{12}$, $1.60 \pm 0.01 \times 10^{12}$, and $1.15 \pm 0.01 \times 10^{12}$ L mol^{-1} s^{-1} at 293, 298, 304, and 310 K, respectively, which were much greater than the maximum scatter collision quenching constant of various quenchers with biopolymers, 2.0×10^{10} L mol^{-1} s^{-1}.[24] These evidence suggested that the probable quenching mechanism of IC by DNA was static quenching.

The fluorescence intensities of IC at different concentrations of DNA were further estimated by the modified Stern−Volmer equation:[25]

$$\frac{F_0}{F_0 - F} = \frac{1}{f_a K_a}\frac{1}{[Q]} + \frac{1}{f_a} \quad (7)$$

where K_a is the modified Stern−Volmer association constant for the accessible fluorophores and f_a is the fraction of accessible fluorescence. The dependence of $F_0/(F_0 - F)$ on the reciprocal value of the quencher concentration $1/[Q]$ is linear, and the constant K_a is the quotient of an ordinate $1/f_a$ and slope $1/f_a K_a$. The values of the association constant K_a for the DNA−IC complex at different temperatures are summarized in Table 1. As shown in Table 1, the decreasing trend of K_a with an increasing temperature was in accordance with the dependence of K_{SV} upon the temperature as discussed above, which further confirmed that the fluorescence quenching of IC was static quenching.

Thermodynamic Analysis. The acting forces between small molecules and biomolecules involve weak interactions, such as hydrogen bond, electrostatic forces, van der Waals forces, and hydrophobic interaction. The thermodynamic parameters of the binding reaction, enthalpy change ($\Delta H°$) and entropy change ($\Delta S°$), are the main evidence for confirming the binding force. If the temperature does not vary distinctly, $\Delta H°$ can be regarded as a constant, and then its value and $\Delta S°$ value can be calculated from the van't Hoff equation as follows:

$$\log K_a = -\frac{\Delta H°}{2.303RT} + \frac{\Delta S°}{2.303R} \quad (8)$$

where R is the gas constant and the temperatures used were 293, 298, 304, and 310 K. The values of $\Delta H°$ and $\Delta S°$ were obtained from the slope and intercept of the linear plot of log K_a versus $1/T$. The value of free energy change ($\Delta G°$) can be obtained from the following equation:

$$\Delta G° = \Delta H° - T\Delta S° \quad (9)$$

The thermodynamic parameters for the interaction of DNA with IC are listed in Table 1. The negative values of $\Delta G°$ revealed the spontaneity of the binding of IC to DNA. The values for $\Delta H°$ and $\Delta S°$ were -23.36 ± 0.02 kJ mol^{-1} and 10.81 ± 0.06 J mol^{-1} K^{-1}, respectively. The positive $\Delta S°$ value is regularly regarded as evidence of the hydrophobic interaction,[26] while the negative value of $\Delta H°$ can be mainly attributed to hydrogen-binding interactions.[27] Thus, both hydrophobic interactions and hydrogen bonds played a predominant role in the binding of IC to DNA and contributed to the stability of the complex.

UV−Vis Absorption Spectroscopic Characteristics. The UV−vis absorption spectra of IC in the absence and presence of different concentrations of DNA are shown in Figure 3. IC exhibited three absorption bands at around 255, 304, and 386 nm, respectively. With increasing amounts of DNA, the absorption intensity of IC at 304 and 386 nm decreased gradually. Moreover, a fairly clear isosbestic point was observed at approximately 294 nm. This observation indicated that a stable DNA−IC complex was formed. The absorption intensity at 255 nm increased significantly, and the absorption peak shifted to 258 nm, which were likely attributed to the spectral overlapping between IC and DNA. The hypochromic effect in UV spectra upon small molecule binding to DNA is a typical characteristic of an intercalating mode.[28] The results implied that the binding mode between IC and DNA might be intercalation.

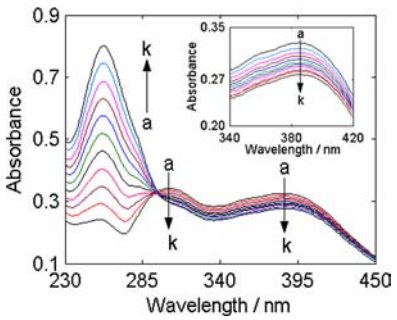

Figure 3. UV−vis absorption spectra of IC varying with different concentrations of DNA at pH 7.4 and room temperature. c(IC) = 6.0×10^{-5} mol L^{-1}, and c(DNA) = 0, 0.638, 1.272, 1.901, 2.526, 3.148, 3.765, 4.378, 4.987, 5.592, and 6.194×10^{-5} mol L^{-1}, corresponding to the curves from a to k, respectively.

Fluorescence Polarization Analysis. Polarization is an important parameter of fluorescence. The polarization value of the small molecule is very low because of the rapid tumbling

motion of the molecule in aqueous media. When the molecule intercalates into the helix of DNA, its rotational motion is restricted, and therefore, the fluorescence polarization of the bound chromophore should be increased.[29] Merely binding to the phosphate backbone or DNA grooves does not result in a significant enhancement of the fluorescence polarization.[30] Fluorescence polarization can be obtained from the following equation:[29]

$$P = \frac{I_{VV} - GI_{VH}}{I_{VV} + GI_{VH}} \quad (10)$$

where I_{VV} and I_{VH} are the emission intensities obtained with the excitation polarizer oriented vertically and emission polarizer oriented vertically and horizontally, respectively. G is the instrument grating correction factor, $G = I_{HV}/I_{HH}$, where I_{HV} is the vertical polarization intensity parallel with excitation and I_{HH} is the horizontal polarization intensity parallel with excitation. Figure 4 shows that the fluorescence of IC was

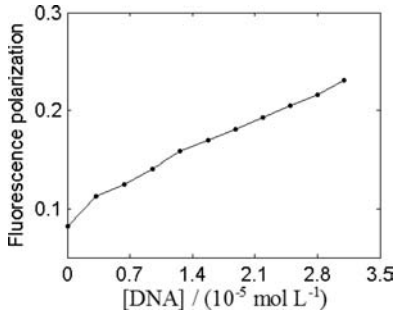

Figure 4. Effect of the DNA concentration on fluorescence polarization of IC at pH 7.4 and room temperature (λ_{ex} = 280 nm, and λ_{em} = 322 nm). c(IC) = 6.0 × 10^{-5} mol L^{-1}.

weakly polarized in the absence of DNA but the fluorescence polarization was increased gradually with the increase in the DNA concentration, which illustrated that IC intercalated into the helix of DNA.

Comparison of the Interactions of IC to ssDNA and dsDNA. To understand the binding mode of IC and DNA, the fluorescence quenching effect of both ssDNA and dsDNA on IC was studied. When a small molecule interacted with the phosphate groups of DNA, whether ssDNA or dsDNA, the quenching effect should be the same. If the binding mode was intercalation, the quenching effect of ssDNA should be weaker than that of dsDNA for the release of the double strands of DNA.[31] If there was a groove binding, the quenching effect of ssDNA should be strengthened in comparison to dsDNA.[32] As shown in Figure 5, both dsDNA and ssDNA could quench the fluorescence of IC and the values of K_{SV} for dsDNA and ssDNA were calculated to be 2.24 ± 0.01 × 10^4 and 1.84 ± 0.01 × 10^4 L mol^{-1}, respectively. The quenching effect of dsDNA was stronger than that of ssDNA, implying that there is an intercalating interaction between IC and DNA.

Iodide Quenching Studies. Further evidence for the intercalative binding of IC to DNA was obtained through iodide quenching experiments. A highly negatively charged quencher was expected to be repelled by the negatively charged phosphate backbone of DNA. Therefore, for an intercalative binding, small molecules should be protected from being quenched by an anionic quencher.[33] In contrast, the free aqueous complex or groove binding molecule should be

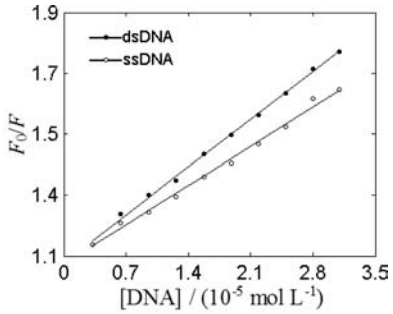

Figure 5. Fluorescence quenching plots of IC by dsDNA and ssDNA at pH 7.4 and room temperature. c(IC) = 6.0 × 10^{-5} mol L^{-1}.

quenched readily by an anionic quencher. As a result, the value of quenching constants (K_{SV}) of the intercalative bound molecule should be lower than that of the free small molecule, and the magnitude of K_{SV} of the molecule bound to DNA by groove binding should be higher than that of the free small molecule.[34] The negatively charged I^- was selected for this purpose. The values of K_{SV} for free IC and the bound IC with DNA by the I^- ion were obtained to be 90.95 ± 0.03 and 40.62 ± 0.01 L mol^{-1}, respectively, using the Stern−Volmer equation (shown in Figure 6). The apparent change in the iodide quenching effect was observed when IC interacted with DNA, which indicated that IC molecules bound to DNA through the intercalative binding.

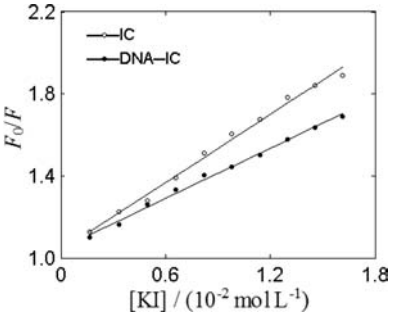

Figure 6. Stern−Volmer plots for the quenching of IC by KI in the absence and presence of DNA at pH 7.4 and room temperature. c(IC) = 6.0 × 10^{-5} mol L^{-1}, and c(DNA) = 1.263 × 10^{-5} moL L^{-1}.

Viscosity Measurements. The viscosity experiment is considered as one of the most unambiguous methods in clarifying the binding mode of a small molecule and DNA. A classical intercalation binding demands the space of adjacent base pairs to be large enough to accommodate the bound ligand and to elongate the double helix, resulting in a significant increase in the DNA viscosity.[19] In contrast, a partial or non-classical intercalation of ligand could bind kinking or bending the double helix, reducing the viscosity of DNA. Besides, the non-intercalation binding, such as electrostatic and grooved face mode, has a smaller effect on viscosity.[35] Figure 7 represents that the relative viscosity of DNA remarkably increased upon the addition of IC, which was similar to the increasing trend of DNA viscosity with increasing concentrations of EB, a typical DNA intercalator. Such a distinct behavior provided strong evidence for the intercalative binding of IC with the DNA, which convincingly supported the conclusion above.

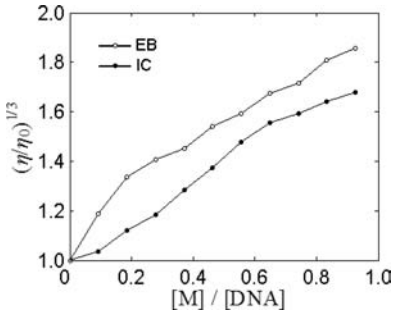

Figure 7. Effect of increasing amounts of IC on the relative viscosity of DNA at pH 7.4. c(DNA) = 3.6 × 10^{-5} mol L^{-1}.

DNA-Melting Analysis. The melting temperature (T_m) of DNA, which is defined as the temperature at which half of the dsDNA is dissociated into single strands, is strictly related to the stability of the macromolecule. In addition, the melting temperature of DNA may be altered by the interaction with chemicals. In general, the intercalation of small molecules into the double helix can increase the stability of the DNA helical structure and lead to the T_m of DNA increase of about 5−8 °C, while the non-intercalation binding causes no visible enhancement in T_m.[36] The melting curves of DNA and the DNA−IC system are shown in Figure 8. As seen from Figure 8, the T_m

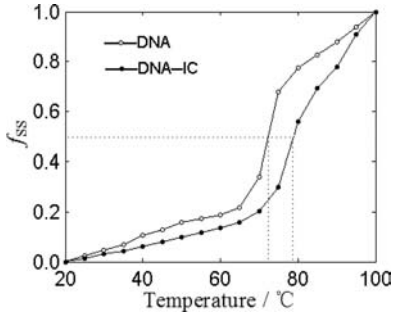

Figure 8. Melting curves of DNA in the absence and presence of IC at pH 7.4. c(IC) = 3.6 × 10^{-5} mol L^{-1}, and c(DNA) = 3.6 × 10^{-5} mol L^{-1}.

values of DNA in the absence and presence of IC were 72.5 and 79.0 °C, respectively, indicating that the stability of DNA was increased in the presence of IC. The results also strongly supported by the intercalative binding of IC with DNA.

CD Studies. CD is a useful technique to monitor changes in DNA morphology following ligand−DNA interactions, owing to its sensitivity to the subtle variations of DNA chiral conformation.[37] The CD spectra of DNA were recorded in the presence of increasing amounts of IC, and the molar ratios of [IC]/[DNA] were 0, 1, and 2 (Figure 9). It was obvious that DNA had the characteristic CD signal in the UV region, one positive band at 278 nm because of the base stacking and one negative band at 246 nm because of the right-handed B-form helicity,[38] while IC was almost non-signal under the same experimental conditions. The intensities of the negative band decreased (shifting to zero levels) accompanied by a slight blue shift about 1 nm, while the positive band decreased remarkably without any significant shift in the band position upon the interaction with IC. These results suggested the effect of intercalation of IC into base stacking and a decreased right-handedness of the DNA as well.[39,40]

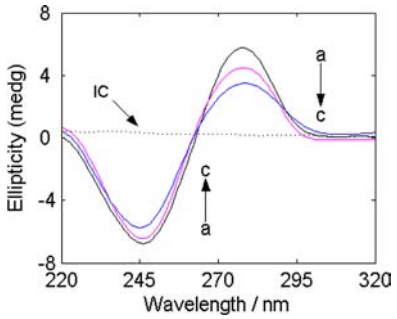

Figure 9. CD spectra of DNA in the presence of increasing amounts of IC at pH 7.4 and room temperature. c(DNA) = 6.0 × 10^{-4} mol L^{-1}. The molar ratios of IC/DNA were (a) 0:1, (b) 1:1, and (c) 2:1.

Synchronous Fluorescence Spectra of the Interaction between IC and DNA−EB. EB, one of the most sensitive fluorescence probes, has a planar structure that binds DNA by an intercalative mode.[41] It has been normally used to probe the DNA structure upon a small molecule or protein interaction. Generally, EB has poor fluorescence efficiency in aqueous medium, but the fluorescence intensity is greatly enhanced upon the addition of DNA.[42] In this work, it was found that IC had no effect on the fluorescence intensity and peak position of EB. Consequently, EB was adopted as the fluorescence probe to investigate the interaction of IC with DNA through the synchronous fluorescence experiments. The molar ratio ([DNA]/[EB]) of 11 was selected in this study (in this case, the fluorescence intensity of EB did not further increase upon sequentially adding DNA to EB solution).

The synchronous fluorescence spectra of the DNA−EB complex in the absence and presence of IC are displayed in Figure 10. The fluorescence intensity of the DNA−EB complex

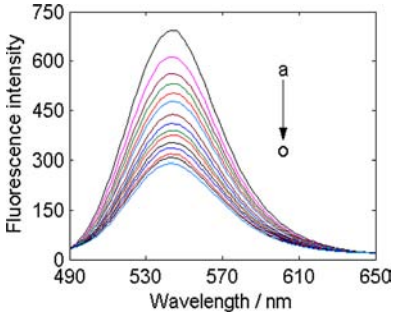

Figure 10. Synchronous fluorescence spectra of the competition between IC and EB with DNA. c(EB) = 5.0 × 10^{-6} mol L^{-1}, c(DNA) = 5.5 × 10^{-5} mol L^{-1}, and c(IC) = 0, 0.498, 0.993, 1.485, 1.974, 2.459, 2.941, 3.420, 3.896, 4.369, 4.839, 5.305, 5.769, 6.230, and 6.688 × 10^{-5} mol L^{-1}, corresponding to the curves from a to o, respectively. $\Delta\lambda$ = 60 nm.

at 545 nm decreased markedly, and the peak shifted to 542 nm with the increase of the IC concentration, indicating that some of the EB molecules, which were intercalated into the DNA base pairs, were replaced by IC and released into the aqueous medium. That is to say, the competitive binding interaction between IC and EB with DNA occurred.

Analysis of the Three-Way Synchronous Fluorescence Spectra of IC, EB, and DNA−EB. In general, fluorescence spectroscopy has been applied in many chemical-related fields. However, the presence of Rayleigh and Raman light scattering phenomena interfere with and complicate the analysis of the

classical fluorescence measurements. The synchronous fluorescence spectroscopy is an approach that can eliminate or reduce this problem significantly.[43]

In most synchronous spectroscopy studies of chemical systems, the selection of $\Delta\lambda$ is particularly important, because the values of $\Delta\lambda$ can substantially influence the shape, location, and signal intensity of a fluorescence peak.[44] To estimate the optimal value of $\Delta\lambda$ and to investigate the chemical system thoroughly, the three-way synchronous fluorescence spectra for IC, EB, and the DNA−EB complex were measured, respectively. The contour plots produced from such three-way data showed that the preferred $\Delta\lambda$ for the three systems was indeed different, with the values of 45, 110, and 70 nm for IC, EB, and DNA−EB, respectively (arrows in Figure 11). It

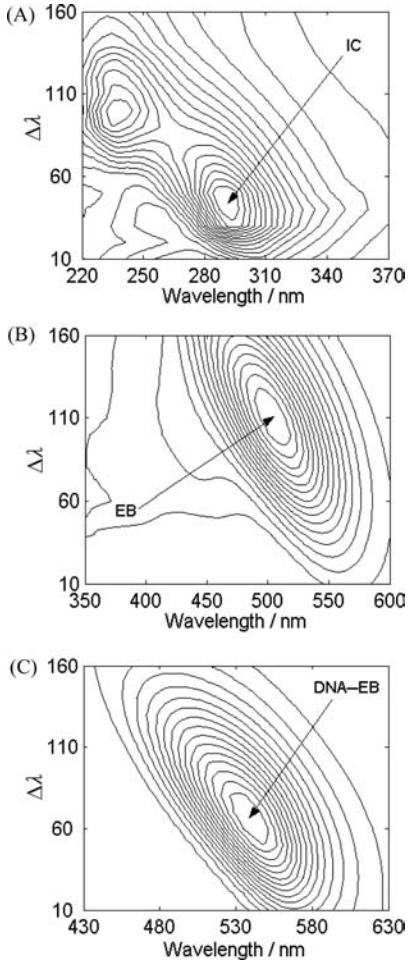

Figure 11. Synchronous fluorescent spectra (contour mode) and the selection of the preferred value of $\Delta\lambda$ for (A) IC, (B) EB probe, and (C) DNA−EB complex.

can obviously be seen that the fluorescence intensity and peak position varied with the different values of $\Delta\lambda$. Therefore, the advantage of the three-way approach became apparent. With the conventional two-way synchronous fluorescence methodology, where $\Delta\lambda$ is fixed at one value, errors will clearly arise in any simultaneous investigation of IC, EB, and DNA−EB complex systems. These errors may be avoided using the three-way synchronous fluorescence method for the selection of $\Delta\lambda$ values.

Decomposition of the Three-Way Synchronous Fluorescence Spectra by PARAFAC. Recently, the three-way synchronous fluorescence spectroscopy combined with PARAFAC modeling has been successfully applied for quantitative analysis of complex systems.[45] To evaluate the competitive interactions of the complicated system consisting of IC, EB, and DNA and to understand their states at equilibrium, the three-component PARAFAC algorithm was applied. The experimental solutions were prepared at the chosen concentrations, as described above in the Fluorescence Measurements section. When food colorant IC with 14 different concentrations was added sequentially to a solution of DNA−EB, a total of 14 two-way data matrices were produced. These data were then arranged into a three-dimensional (3D) array stack [$\Delta\lambda$ (A way)−excitation wavelength (B way)−sample (C way)]. This matrix of $\boldsymbol{X}$ (20 × 501 × 14) was decomposed into the loading matrices, $\boldsymbol{A}$, $\boldsymbol{B}$, and $\boldsymbol{C}$, with the use of the PARAFAC method.

Excitation loadings (matrix $\boldsymbol{B}$ in Figure 12A, solid line) indicated that the resolved excitation spectra for these three

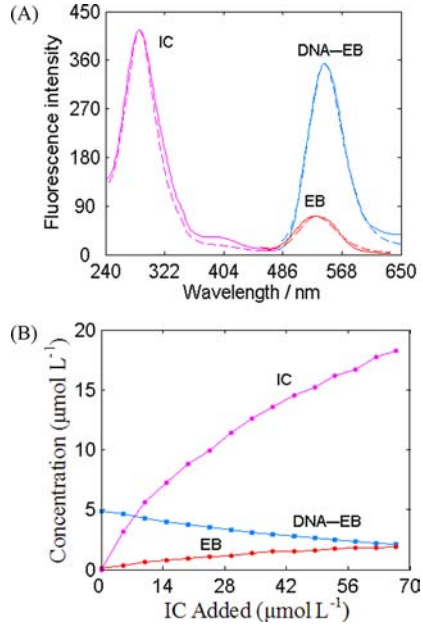

Figure 12. (A) Comparison of the measured excitation synchronous fluorescence spectra for IC, EB, and the DNA−EB complex with those resolved from PARAFAC: (—) resolved spectra from PARAFAC and (- - -) measured spectra. (B) Equilibrium concentrations of IC, EB, and the DNA−EB complex resolved by the PARAFAC model.

species, IC, EB, and the DNA−EB complex, were quite similar to the measured counterparts (Figure 12A, dashed line). This suggested that the results obtained from PARAFAC were unique and reliable and that the correct number of components was chosen. Furthermore, the extracted loadings from the spectra were used to estimate the state of equilibrium. The relative equilibrium concentrations of IC, EB, and the DNA−EB complex resolved by the PARAFAC model (the rows in the loading matrix $\boldsymbol{C}$ in Figure 12B) can be considered to reflect the real reacting fluorescing species studied in the system because PARAFAC only gives unique solutions.

It can be observed from Figure 12B that the concentration of the DNA−EB complex decreased gradually accompanied by the increase of the concentration of EB with the addition of IC. The displacement of EB in the DNA−EB complex by IC can be visualized clearly, indicating that IC intercalated into the same

base sites of DNA, releasing the bound EB. PARAFAC further demonstrated the intercalation binding of IC to the DNA.

In summary, the interaction between IC and DNA in pH 7.4 Tris-HCl buffer solution was studied using EB as a probe by UV−vis absorption, fluorescence, and CD spectroscopy, as well as viscosity measurements and DNA-melting studies. The results suggested that the fluorescence of IC was quenched significantly by DNA and the probable quenching mechanism was a static quenching procedure. The binding mode of IC to DNA was an intercalation binding, which was supported by the results from fluorescence polarization experiments, iodide fluorescence quenching effect, ssDNA quenching effect, viscosity assays, and DNA-melting measurements. The association constant (K_a) value between IC and DNA was in the order of 10^4 L mol^{-1}, which was similar to other reported DNA intercalators, such as butylated hydroxyanisole (BHA),[46] dinitrogen Schiff base (SF),[47] and 2-*tert*-butylhydroquinone (TBHQ).[48] The thermodynamic parameters, ΔH° and ΔS°, were calculated to be -23.36 ± 0.02 kJ mol^{-1} and 10.81 ± 0.06 J mol^{-1} K^{-1}, respectively, indicating that the binding of IC to DNA was driven mainly by hydrophobic interactions and hydrogen bonds. Moreover, PARAFAC was applied to resolve three-way synchronous fluorescence data array of the interaction between IC and EB with DNA, and the obtained results indicated the intercalation of IC molecules into the double helix of DNA by substituting for the EB probe. It should be noted that the concentration (6.0×10^{-5} mol L^{-1}) of IC that was used in this study was much less than that currently being used as a food additive. Consequently, it is worth making a thorough analysis on its widespread usage in the food industry.

AUTHOR INFORMATION

Corresponding Author

*Telephone: +8679188305234. Fax: +8679188304347. E-mail: gwzhang@ncu.edu.cn.

Funding

This study was supported financially by the National Natural Science Foundation of China (21167013 and 31060210), the Natural Science Foundation of Jiangxi Province (20114BAB204019), the Open Project Program and Objective-Oriented Project of the State Key Laboratory of Food Science and Technology of Nanchang University (SKLF-KF-201203 and SKLF-MB-201002), and the Foundation of Jiangxi Provincial Office of Education (GJJ11287).

Notes

The authors declare no competing financial interest.

REFERENCES

(1) Khera, K. S.; Munro, I. C.; Radomski, J. L. A review of the specifications and toxicity of synthetic food colors permitted in Canada. *Crit. Rev. Toxicol.* **1979**, *6*, 81−133.

(2) Lakshmi, U. R.; Srivastava, V. C.; Mall, I. D.; Lataye, D. H. Rice husk ash as an effective adsorbent: Evaluation of adsorptive characteristics for indigo carmine dye. *J. Environ. Manage.* **2009**, *90*, 710−720.

(3) Barka, N.; Assabbane, A.; Nounah, A.; Ichou, Y. A. Photocatalytic degradation of indigo carmine in aqueous solution by TiO_2-coated non-woven fibres. *J. Hazard. Mater.* **2008**, *152*, 1054−1059.

(4) Secula, M. S.; Creţescu, I.; Petrescu, S. An experimental study of indigo carmine removal from aqueous solution by electrocoagulation. *Desalination* **2011**, *277*, 227−235.

(5) Mittal, A.; Mittal, J.; Kurup, L. Batch and bulk removal of hazardous dye, indigo carmine from wastewater through adsorption. *J. Hazard. Mater.* **2006**, *137*, 591−602.

(6) Ni, Y. N.; Wei, M.; Kokot, S. Electrochemical and spectroscopic study on the interaction between isoprenaline and DNA using multivariate curve resolution-alternating least squares. *Int. J. Biol. Macromol.* **2011**, *49*, 622−628.

(7) Arakawa, H.; Ahmad, R.; Naoui, M.; Tajmir-Riahi, H. A. A comparative study of calf thymus DNA binding to Cr(III) and Cr(VI) ions. *J. Biol. Chem.* **2000**, *275*, 10150−10153.

(8) Kashanian, S.; Zeidali, S. H. DNA binding studies of tartrazine food additive. *DNA Cell Biol.* **2011**, *30*, 499−505.

(9) Kalanur, S. S.; Katrahalli, U.; Seetharamappa, J. Electrochemical studies and spectroscopic investigations on the interaction of an anticancer drug with DNA and their analytical applications. *J. Electroanal. Chem.* **2009**, *636*, 93−100.

(10) Kashanian, S.; Javanmardi, S.; Chitsazan, A.; Paknejad, M.; Omidfar, K. Fluorometric study of fluoxetine DNA binding. *J. Photochem. Photobiol., B* **2012**, *113*, 1−6.

(11) Tong, C. L.; Xiang, G. H.; Bai, Y. Interaction of paraquat with calf thymus DNA: A terbium(III) luminescent probe and multispectral study. *J. Agric. Food. Chem.* **2010**, *58*, 5257−5262.

(12) Jangir, D. K.; Charak, S.; Mehrotra, R.; Kundu, S. FTIR and circular dichroism spectroscopic study of interaction of 5-fluorouracil with DNA. *J. Photochem. Photobiol., B* **2011**, *105*, 143−148.

(13) Guo, H. Q.; Cai, C. Q.; Gong, H.; Chen, X. M. Multi-spectroscopic method study the interaction of anti-inflammatory drug ketoprofen and calf thymus DNA and its analytical application. *Spectrochim. Acta, Part A* **2011**, *79*, 92−96.

(14) Oehlers, L.; Mazzitelli, C. L.; Brodbelt, J. S.; Rodriguez, M.; Kerwin, S. Evaluation of complexes of DNA duplexes and novel benzoxazoles or benzimidazoles by electrospray ionization mass spectrometry. *J. Am. Soc. Mass Spectrom.* **2004**, *15*, 1593−1603.

(15) Ni, Y. N.; Lin, D. Q.; Kokot, S. Synchronous fluorescence and UV−vis spectrometric study of the competitive interaction of chlorpromazine hydrochloride and neutral red with DNA using chemometrics approaches. *Talanta* **2005**, *65*, 1295−1302.

(16) Kanakis, C. D.; Nafisi, Sh.; Rajabi, M.; Shadaloi, A.; Tarantilis, P. A.; Polissiou, M. G.; Bariyanga, J.; Tajmir-Riahi, H. A. Structural analysis of DNA and RNA interactions with antioxidant flavonoids. *Spectroscopy* **2009**, *23*, 29−43.

(17) Jangir, D. K.; Tyagi, G.; Mehrotra, R.; Kundu, S. Carboplatin interaction with calf-thymus DNA: A FTIR spectroscopic approach. *J. Mol. Struct.* **2010**, *969*, 126−129.

(18) Steiner, R. F.; Weinryb, L. *Excited States of Protein and Nucleic Acid*; Plenum Press: New York, 1971; p 40.

(19) Grueso, E.; López-Pérez, G.; Castellano, M.; Prado-Gotor, R. Thermodynamic and structural study of phenanthroline derivative ruthenium complex/DNA interactions: Probing partial intercalation and binding properties. *J. Inorg. Biochem.* **2012**, *106*, 1−9.

(20) Zhao, P.; Huang, J. W.; Mei, W. J.; He, J.; Ji, L. N. DNA binding and photocleavage specificities of a group of tricationic metalloporphyrins. *Spectrochim. Acta, Part A* **2010**, *75*, 1108−1114.

(21) Harshman, R. A.; Lundy, M. E. PARAFAC: Parallel factor analysis. *Comput. Stat. Data Anal.* **1994**, *18*, 39−72.

(22) Bro, R. Exploratory study of sugar production using fluorescence spectroscopy and multi-way analysis. *Chemom. Intell. Lab. Syst.* **1999**, *46*, 133−147.

(23) Shahabadi, N.; Maghsudi, M.; Kiani, Z.; Pourfoulad, M. Multispectroscopic studies on the interaction of 2-*tert*-butylhydroquinone (TBHQ), a food additive, with bovine serum albumin. *Food Chem.* **2011**, *124*, 1063−1068.

(24) Lakowicz, J. R; Weber, G. Quenching of fluorescence by oxygen: A probe for structural fluctuations in macromolecules. *Biochemistry* **1973**, *12*, 4161−4170.

(25) Zhang, G. W.; Zhao, N.; Wang, L. Fluorescence spectrometric studies on the binding of puerarin to human serum albumin using warfarin, ibuprofen and digitoxin as site markers with the aid of chemometrics. *J. Lumin.* **2011**, *131*, 2716−2724.

(26) Ross, P. D.; Subramanian, S. Thermodynamics of protein association reaction: Forces contributing to stability. *Biochemistry* **1981**, *20*, 3096−3102.
(27) Zhang, G. W.; Wang, L.; Pan, J. H. Probing the binding of the flavonoid diosmetin to human serum albumin by multispectroscopic techniques. *J. Agric. Food. Chem.* **2012**, *60*, 2721−2729.
(28) Lu, Y.; Lv, J.; Zhang, G. S.; Wang, G. K.; Liu, Q. F. Interaction of an anthracycline disaccharide with ctDNA: Investigation by spectroscopic technique and modeling studies. *Spectrochim. Acta, Part A* **2010**, *75*, 1511−1515.
(29) Cui, F. L.; Hui, G. Q.; Jiang, X. Y.; Zhang, G. S. Interaction of 3′-azido-3′-deamino daunorubicin with DNA: Multispectroscopic and molecular modeling. *Int. J. Biol. Macromol.* **2012**, *50*, 1121−1126.
(30) Li, J. F.; Li, B. H.; Wu, Y. B.; Shuang, S. M.; Dong, C.; Choi, M. M. F. Luminescence and binding properties of two isoquinoline alkaloids chelerythrine and sanguinarine with ctDNA. *Spectrochim. Acta, Part A* **2012**, *95*, 80−85.
(31) Catalán, M.; Álvarez-Lueje, A.; Bollo, S. Electrochemistry of interaction of 2-(2-nitrophenyl)-benzimidazole derivatives with DNA. *Bioelectrochemistry* **2010**, *79*, 162−167.
(32) Cai, C. Q.; Chen, X. M.; Ge, F. Analysis of interaction between tamoxifen and ctDNA in vitro by multi-spectroscopic methods. *Spectrochim. Acta, Part A* **2010**, *76*, 202−206.
(33) Kashanian, S.; Khodaei, M. M.; Pakravan, P. Spectroscopic studies on the interaction of isatin with calf thymus DNA. *DNA Cell Biol.* **2010**, *29*, 639−646.
(34) Kumar, C. V.; Turner, R. S.; Asuncion, E. H. Groove binding of a styrylcyanine dye to the DNA double helix: The salt effect. *J. Photochem. Photobiol., A* **1993**, *74*, 231−238.
(35) Bera, R.; Sahoo, B. K.; Ghosh, K. S.; Dasgupta, S. Studies on the interaction of isoxazolcurcumin with calf thymus DNA. *Int. J. Biol. Macromol.* **2008**, *42*, 14−21.
(36) Qiao, C. Y.; Bi, S. Y.; Sun, Y.; Song, D. Q.; Zhang, H. Q.; Zhou, W. H. Study of interactions of anthraquinones with DNA using ethidium bromide as a fluorescence probe. *Spectrochim. Acta, Part A* **2008**, *70*, 136−143.
(37) Ivanov, V. I.; Minchenkova, L. E.; Schyolkina, A. K.; Poletayev, A. I. Different conformations of double-stranded nucleic acid in solution as revealed by circular dichroism. *Biopolymers* **1973**, *12*, 89−110.
(38) Barone, G.; Gambino, N.; Ruggirello, A.; Silvestri, A.; Terenzi, A.; Liveri, V. T. Spectroscopic study of the interaction of Ni^{II}-5-triethyl ammonium methyl salicylidene *ortho*-phenylendiiminate with native DNA. *J. Inorg. Biochem.* **2009**, *103*, 731−737.
(39) Xu, X. Y.; Wang, D. D.; Sun, X. J.; Zeng, S. Y.; Li, L. W.; Sun, D. Z. Thermodynamic and spectrographic studies on the interactions of ct-DNA with 5-fluorouracil and tegafur. *Thermochim. Acta* **2009**, *493*, 30−36.
(40) Zhang, G. W.; Fu, P.; Wang, L.; Hu, M. M. Molecular spectroscopic studies of farrerol interaction with calf thymus DNA. *J. Agric. Food. Chem.* **2011**, *59*, 8944−8952.
(41) Lepecq, J. B.; Paoletti, C. A fluorescent complex between ethidium bromide and nucleic acids: Physical−chemical characterization. *J. Mol. Biol.* **1967**, *27*, 87−106.
(42) Zou, H. Y.; Wu, H. L.; Zhang, Y.; Li, S. F.; Nie, J. F.; Fu, H. Y.; Yu, R. Q. Studying the interaction of pirarubicin with DNA and determining pirarubicin in human urine samples: Combining excitation−emission fluorescence matrices with second-order calibration methods. *J. Fluoresc.* **2009**, *19*, 955−966.
(43) Lloyd, J. B. F. Synchronized excitation of fluorescence emission spectra. *Nature* **1971**, *231*, 64−65.
(44) Andersen, C. M.; Bro, R. Practical aspects of PARAFAC modeling of fluorescence excitation−emission data. *J. Chemom.* **2003**, *17*, 200−215.
(45) Nikolajsen, R. P. H.; Booksh, K. S.; Hansen, Å. M.; Bro, R. Quantifying catecholamines using multi-way kinetic modeling. *Anal. Chim. Acta* **2003**, *475*, 137−150.
(46) Kashanian, S.; Dolatabadi, J. E. N. In vitro study of calf thymus DNA interaction with butylated hydroxyanisole. *DNA Cell Biol.* **2009**, *28*, 589−596.
(47) Shahabadi, N.; Kashanian, S.; Darabi, F. In vitro study of DNA interaction with a water-soluble dinitrogen schiff base. *DNA Cell Biol.* **2009**, *28*, 535−540.
(48) Kashanian, S.; Dolatabadi, J. E. N. DNA binding studies of 2-*tert*-butylhydroquinone (TBHQ) food additive. *Food Chem.* **2009**, *116*, 743−747.